Feasibility study of a spouted bed gasification plant

Authors:
Daniele Bernocco[**], Barbara Bosio, Elisabetta Arato

University of Genoa, DICCA - Depart of Civil Chemical and Environmental Engineering, 15, O. Pia st., 16145 Genoa Italy

Abstract
We have studied the feasibility of building a biomass gasification plant with an innovative spouted bed reactor for distributed energy production. The process was simulated using a thermodynamic approach (concentrated parameter model) using LIBPF, a C++ process modelling library. A nominal size of about 100kW total thermal power was chosen.

Fifteen chemical species were taken into account (dry and ash-free (daf) biomass, C, CH_4, CO, CO_2, H_2, H_2O, N_2, NH_3, O_2, methanol, ethylene, phenol, naphthalene and ash).

After preliminary simulation trials and unit operation sizing, a proper plant configuration was developed.

The air ER (equivalent ratio), syngas condensate recycling and biomass moisture fraction were studied in compliance with the constraint of the gas flow required for a stable spouting regime (120 m^3/h) and optimal gasification temperature (930°C).

A working condition map was obtained in terms of air ER and syngas condensate recycling for different biomass moisture fractions and the main plant performance parameters were studied.

The net electrical yield was found to vary from the ideal maximum of 25% to a minimum of about 17% and the heat cogeneration yield was found to vary in the range 45-48% for all the process conditions studied.

[**] Corresponding author:
Tel. +39 010 353 6504
Fax +39 010 353 2589
E-mail: bernocco.daniele@tiscali.it

1 Introduction

Today world energy consumption is about $12.5x10^9$ toe, about three times that of 40 years ago (IEA 2011), and it is still increasing, demonstrating that energy production is one of the most important demands in all industrialized countries (such as the those of Europe and the USA) and industrializing ones (such as China and India). Economic and pollution problems, fossil fuel limitation and quality of life are all linked to the issue of energy production. A good strategy is important to meet the current growth in energy consumption, political stability and environmental problems. In this scenario, renewable energy sources have a central role and the present work is dedicated to the study of biomass as an energy source feedstock for an innovative thermochemical process.

Obtaining energy from biomass in a safe way could reduce dependence on fossil fuels and energy importation, reduce damage to the environment, achieve the goal of a zero carbon foot print, enhance the use of energy refuse and residues, the return of abandoned energy sites to agricultural production (for energy crops), and create new business and occupational opportunities.

The biomass considered in this work is wood chips, which are suitable for high-temperature thermochemical processes such as pyrolysis, gasification and combustion (Milne et al. 1998, Higman and Burgt 2003 and Goyal et al. 2008).

In terms of gas feed, gasification can be seen as a compromise between endothermic pyrolysis and exothermic combustion, but it is a process that requires fine tuning of operating conditions and feeding compositions. One parameter that is commonly introduced is the *equivalent ratio (ER)*, the oxidizing agent fed (air in the present work) in relation to the oxidizing agent required for the stoichiometric combustion of the condensed matter (dry biomass in the present work). Using this definition, pyrolysis is a zero ER process, while combustion has an ER equal to or greater than 1.

Gasification has an ER between 0 and 1 and its value is fundamental to the efficiency optimization of the gasification process.

In this paper we present the results of a feasibility study of a biomass gasification plant with an innovative spouted bed reactor. The process was simulated through a thermodynamic approach using LIBPF, a C++ process modelling library. After a first simulation trial, a preliminary sizing of the plant was performed, revealing that the spouting regime of the gasifier imposed important constraints. A proper plant configuration was then developed and the main sensitivities were checked to study the optimal process conditions and performance.

2 The spouted bed

Gasification reactors, named *gasifiers*, are usually classified according to their solid handling characteristics. In order of increasing cost, complexity, efficiency and typical sizes, there are moving bed (downdraft and updraft), fluidized bed, bubbling fluidized bed and entrained flow gasifiers (Higman and Burgt 2003).

In the present work we introduce an innovative application of spouted bed reactors. The spouted bed is a specific type of fluidized bed able to produce a good fluid-solid interaction. While in a standard fluidized bed, a fluid is passed through a uniform distributor plate to float the particles which move up and down in groups; in a spouted bed, instead, gas (or occasionally a liquid) is injected vertically upwards through a single central orifice into a bed of granular solid, expanding it. If the flow rate of the fluid and the pressure drop are sufficient and the bed depth is less than the “maximum spoutable bed depth”, the central jet breaks through the upper surface, resulting in a characteristic flow pattern known as spouting.

The high fluid velocity causes a stream of solid particles to rise rapidly in a hollow central core within the bed, with high void fraction (~85%). The central core is called a “spout”, the peripheral

annular region an “annulus” and the mushroom-shaped zone above the annulus a “fountain” (figure 1). The particles, having passed through the bed, fall back onto the annular space between the spout and the container wall forming a fountain, and then slowly travel downwards and, to some extent, inwards in a loosely packed bed. As the fluid travels upwards, it flares out into the annulus, which has a lower void fraction (40-50%) (Markowski and Kaminski 1983, Bi 2004, Anabtawi et al. 2005, Salam and Bhattacharya 2006 a, Salam and Bhattacharya 2006 b).

Figure 1: Spouted bed working scheme

Spouted beds are the focus of renewed attention for physical and chemical operations that require handling of solids for which fluidized beds present problems because of their great size, irregular texture, or sticky nature, as is the case of combustion of vegetable biomass or bituminous coal, pyrolysis of vegetable biomass, pyrolysis of waste plastics, and catalytic polymerizations *(Markowski and Kaminski 1983, Bilbao et al 1987, Rovero and Watkinson 1990, Zahed and Epstein 1992, Olazar et al 1994, Aguado et al 2000, Olazar,et al 2000, Rasul 2001, San Josè et al. 2004, Cui and Grace 2007, Cui and Grace 2008, Amutio et al 2012 and Arabiourrutia et al 2012).*

In addition, spouted beds are of special relevance to biomass particle processing (drying, toasting, pyrolysis, gasification and combustion). Some studies (Olazar et al. 1994) have demonstrated that spouted beds are quite good for A, B and D particle types of the well known Geldart’s classification (Geldart 1973). *Moreover, compared to standard fluidized beds, the spouted beds, and especially the dilute conical spouted beds, are suitable for avoiding defluidization due to bed agglomeration (Aguado et al. 2005).*

Gasification requires the development of technical processes that allow biomass particles to be spouted effectively with high gas-solid contact efficiency, high heat and mass transfer rates, as little flow of spouting gas as possible, high solid handling capacity, low particle entrainment and the shortest possible processing time. Gasification of solid fuels in a spouted bed, which has certain

potential advantages over other fluid bed configurations, appears to be an under-exploited technique so far (Salam and Bhattacharya 2006 b).

While gasification in a fixed bed can be considered as occurring in four different reaction zones (drying, pyrolysis, reduction and combustion) in a plug or sequential manner, in fluidized or spouted bed gasifiers separate reaction zones do not exist because of better mixing. All the processes of drying, pyrolysis, reduction and combustion can be regarded as taking place simultaneously throughout the reactor volume although the intensity of any particular process may vary according to its location (Salam and Bhattacharya 2006 b).

3 Modelling approach

In order to study high-temperature biomass-to-energy processes and simulate them, it is important to develop a proper modelling strategy. In this work, the thermodynamic approach was used and thus, concentrated parameter models, such as perfectly mixed volumes, were developed.

Properly-customized, perfectly-mixed units can model gasifiers, heat exchangers, blowers, pumps, mixers, condensers and internal combustion engines or fuel cells. Thus, the process can be modelled by suitably combining these units.

Although spouted bed are characterized by short residence time for the gas phase, we assume that thermodynamic equilibrium was reached in the gasifier, in view of the scopes of the present work, which are the study and the evaluation of the whole process and the survey of the main issues regarding it.

3.1 Simulation tool

The chosen simulation tool was LIBPF™ 1.0 (LIBrary for Process Flowsheeting), Greppi 2006, a process flow-sheeting and modelling tool arranged as a C++ library.

The approach proposed in this chapter has been developed in the C++ programming language and in accordance with the implementation structure of the LIBPF library. The required low-level concepts are components and reactions.

3.2 Components

All main chemical species involved in the process from input to output were taken into account. Each chemical was characterized by its physical (density, composition, etc.) and thermodynamic (specific heat, enthalpy, vapour pressure, etc.) properties. *As exposed in a previous work (Bernocco et al. 2011), fifteen chemical species or components were taken into account in five conceptual component groups: dry and ash-free (daf) biomass, primary components (C, CH_4, CO, CO_2, H_2, H_2O, N_2, NH_3, O_2), secondary components (methanol, ethylene), tertiary components (phenol, naphthalene), and inert/ash component (silica). Although methanol and ethylene are unstable under gasification conditions, the choice of these secondary components is due to the representation of light hydrocarbons with a condensing temperature quite lower than that of water. Similarly, phenol and naphthalene were chosen to represent heavy tars with a condensing temperature higher than water.*

The last four component groups listed above are well-defined chemical species, so they were modelled using their standard LIBPF implementation.

The biomass component requires a different modelling approach because it is not a well-defined chemical specie. The biomass model was developed as a chemical component with constant properties over all the calculations (flow sheet, unit operations, streams) similar to a well defined standard chemical species. Generic biomass is composed of moisture, ash and organic fraction (fixed carbon and volatile matter). Since moisture and ash can be taken into account separately, the biomass model involves only the organic fraction daf.

3.3 Reactions

The chemical species considered are involved in complex chemical transformation within a high-temperature process such as gasification. In this work three groups of chemical reactions were defined, and summarized in Table 1.

Table 1: Chemical reactions considered

The first two types are stoichiometrically defined for well-defined chemical species, while the pyrolysis reaction requires proper modelling of the biomass reactant.

All high-temperature processing of biomasses, such as pyrolysis, gasification and combustion, develop hundreds of chemical species, and the stoichiometric relationship between products and biomass composition is complex to represent (Milne et al. 1998). Moreover the solid does not react directly with the gas phase except for solid carbon (char or coke). The solid biomass always undergoes a first step of pyrolysis or devolatilization (Souza-Santos 2004). A systematic, generic stoichiometric approach to represent a biomass starting material and the repartition of pyrolysis products was developed in a previous work (Bernocco et al. 2011). The approach transforms the conventional representation of the starting organic matter of a biomass into a set of well-defined chemical species while respecting the atomic balances. The complex mixture of the possible gases and condensable products has been simplified (lumped) into 13 components and grouped as primary products (small molecules usually present in the pyrogas or syngas, also under thermodynamic equilibrium conditions), secondary products (light tars with a condensing temperature lower than that of water) and tertiary products (heavy tars with a condensing temperature higher than water).

3.4 Unit operations

Thermodynamic models generally present a system as a zero-dimensional point, with perfect homogeneity and immobility with respect to time. Thus the achievement of thermodynamic equilibrium was assumed.

For these reasons the reactors, such as the gasifier, were modelled as ideal thermodynamic equilibrium reactors.

The power consumption of the blowers was estimated by assuming isentropic compression efficiency equal to 70% and mechanical and electrical efficiencies equal to 90%.

The cyclone was modelled as a perfect gas-solid separator and sized using Stairmand's procedure for high-efficiency cyclones (Sinnott et al. 1999).

The syngas clean-up and cooling-condensing sections were modelled as two cooling units with an estimated pressure drop of 5500 Pa each. An outlet temperature of 130°C was fixed for the first cooler (the clean-up unit): this involves the production of an high temperature usable heat, so that the clean-up unit was considered as a valuable heat cogenerator in the plant efficiency calculations. The syngas cooler-condenser was modelled as a cooling unit with flash vapour-liquid equilibrium with a fixed outlet temperature of 30°C. This unit did not produce usable heat, and so was not included in the plant efficiency calculations.

The power consumption of the pumps was estimated by assuming an electrical efficiency of 85% and a mechanical efficiency of 80%.

The energy conversion section was represented as an internal combustion engine, but modelled as an ideal combustor with outlet temperature fixed at 80°C. The duty of this unit was multiplied by an electricity conversion efficiency of 30% in order to calculate the electrical power production. The remaining duty was multiplied by 75% efficiency in order to calculate the cogeneration heat power of the ICE (Internal Combustion Engine). These efficiency values are commonly accepted for small internal combustion engines, but they can also be extended to other technologies such as gas turbines. Bigger internal combustion engines for stationary combined heat and power generation can reach 48.7% of electrical power efficiency and 41.3% of cogenerating heat efficiency (for a 9.5 MW Jenbacher engine).

3.5 Key spouting parameters

The available literature on spouted beds is mostly based on cylindrical apparatuses with diameters less than 0.3m (Epstein and Grace 2011). Studies of systems of 1m diameter or larger are rare (Cui and Grace 2008). So correlations and models mostly refer to small-scale vessels.

Figure 2: Spouted bed geometry

The properties of spouted bed devices are well described by a few parameters (Becker 1961), which are classifiable into three categories based on dependence. Figure 2 should clarify the geometrical characteristics and the table in Appendix A summarises the major correlations for conical-based spouted beds.

A first parameter category can be considered as involving parameters which depend only on the properties of the gas and particles and the process specifications. It groups the particle terminal settling velocity, hold up and minimum superficial velocity for fluidization.

The terminal settling velocity of free-falling particles under gravity in a stagnant fluid is defined as the velocity at which the drag exerted by the surrounding fluid exactly counterbalances the net gravitational (weight minus buoyancy) force.

The process specifications and average internal conditions give information about hold ups of solid (solid residence time) or about gas hour-space velocity (GHSV). This information usually comes from general kinetic approaches.

The minimum velocity for fluidization is commonly defined as the superficial fluid velocity at which the extrapolated relationship between the frictional pressure drop and the fluid velocity of a quiescent bed intersects the ordinate of equality between the drag and weight forces. The definition is made unique by specifying that the quiescent bed is consolidated by a gradual reduction of agitation.

A second category can be considered as involving parameters that also depend on the column geometry and its groups: inlet and column diameter constraints, maximum spoutable bed height, static and actual bed height and average spout diameter.

The inlet diameter, column diameter and particle size are strictly related to spoutability and stability conditions deriving from experienced observation and experimental studies.

There is a maximum bed depth which can still allow a stable spout. The maximum spoutable bed height is an important parameter in the design of a spouted bed, because it is directly related to the amount of solid that can be processed. Above the maximum spoutable height, the bed enters bubbly and slug flow regimes. Transition to minimum fluidization occurs due to the gas diffusion in the packed bed.

The bed depth can be defined as static or actual. The former comes directly from the solid bulk density and the column geometry. The second can be estimated by using void fractions and spout and fountain sizes. However only experimental proof can correctly evaluate the actual bed height, by measuring the settled bed depth, observed after strongly agitating a bed and then gradually shutting off the gas flow (Becker 1961).

The spout diameter and shape at the bed level are only important at the gas inlet zone of the bed. Consequently, to model the gas and solid flow in spouted beds and for the sake of simplicity, it is useful to assume that the spout diameter is independent of its longitudinal position on the bed (San Jose et al. 2001). Usually, an average value of the diameter, estimated from semi-empirical or theoretical correlations, is taken.

Finally, a third category can be considered as involving parameters that also depend on the bed depth, which is to say that it is related to the residence times of the gas or solid. This category groups the minimum and actual spouting velocity, fountain size, maximum bed pressure drop, and stable bed pressure drop.

The minimum spouting velocity is the lowest gas velocity required to make the fountain. The actual spouting velocity can be calculated from the gas feed rate, referring to the inlet section or to the

column section. A slight reduction in the air velocity under this condition causes the spout to collapse and the pressure drop in the bed to rise suddenly. The minimum spouting velocity has been widely studied in literature (Mathur and Epstein 1974, Wu et al. 1987, Ye et al. 1992, Salam and Bhattacharya 2006 a).

The fountain is characterized by a generally paraboloidal external shape. So it can be described by only two parameters: the height and the base surface. The fountain height is a fundamental variable to evaluate the total height of the apparatus, while the base surface is important for the fountain-annulus interaction and for the solid recirculation (Wu et al. 1987, Ye et al. 1992)

The maximum bed-pressure drop is the gas-pressure drop required to start up the spout and it is fundamental for sizing the gas-blowing system.

The stable bed pressure drop is the gas pressure drop required for spouting under a stationary regime.

In order to improve the spouting stability and gas flow rate flexibility, there are some works about the introduction of a draft tube that stabilizes the spout-annulus interface (Altzibar et al. 2008 and Altzibar et al. 2009). In the present work, the draft tube was not considered in order to simplify the spouted bed design.

Considerable information exists on the hydrodynamics of spouted beds and spout-fluidized beds under ambient conditions (Mathur and Epstein 1974, Epstein and Grace 2011). Only a few studies have been conducted on hot spouting from 20 to 400°C (Wu et al. 1987) and from 20 to 880°C (Ye et al. 1992), *applicable to combustion and gasification in conical-based cylindrical spouted beds. Some recent studies were done on high temperature spouting (Olazar et al 2009, Makibar et al. 2011), but they are strictly related to conical spouted beds.*

So there is considerable uncertainty that necessitates care and overdesign in sizing spouted bed gasifiers. Equations originally developed for room-temperature conditions are often applied to high temperatures, with the assumption that these equations will give reasonable predictions if used with gas physical-property values appropriate to the actual operating conditions (Wu et al. 1987).

For the sake of the applicability of the process study, the spouted bed sizing was important because it introduces the constraint of volumetric flow fed to the gasifier and so it requires the proposed recycling configuration.

4 The reference process

In the distributed energy production scenario the smallest plant capacity compatible with technological constraints is preferable. So, in choosing the plant size for our case study, the commercial availability of the biomass feedstock, the present knowledge of the spouted bed and the scope of energy production were considered. In our work, we assumed a nominal size of about 100kW total thermal power, but the results can be generalized to smaller or greater sizes. This value should correspond to a biomass feeding rate of about 20kg/h. Increasing the nominal plant capacity is possible, but not compatible with the aim of distributed energy production. On the other hand, reducing the plant size is not safe for the handling of commercially available feedstocks. It is possible to obtain a very low power-plant size using sawdust. This case involves such a small apparatus that the heat dispersion of the hot devices may undermine the feasibility of the unit operations from a thermal point of view.

In a biomass gasification process, the CBL (Carbon Boundary Limit) delimits, on the basis of thermodynamic equilibrium, the region where solid carbon is all converted in gaseous products. The CBL strongly depends on ER, since the latter influences the system composition by imposing the amount of oxidizing agent. For this reason, the optimization of the ER parameter is very important, as demonstrated by Prins' exergetic analysis (Prins 2005). In this work, after a few model test runs, we found that the best plant performance should be for ER varying between 30% and 50%.

Another important parameter to be taken into account is the gasification temperature. Prins (Prins 2005) has demonstrated that about 927°C must be reached for good reaction kinetics. Thus we adjusted the parameters in order to always reach 930°C in the spouted bed gasifier.

The biomass feedstock considered in this study consisted of wood chips, whose nominal composition was taken from the Phyllis database (ECN 2010) and was averaged as shown in Table 2.

Table 2: Chemical characteristics of the biomasses (ECN 2010).
HHV = higher heating value, LHV = lower heating value,
M = moisture, VM = volatile matter, A = ash, FC = fixed carbon,
ar = as received basis, dry = moisture-free basis, daf = dry and free ash.

Commercially available wood chips are sold in four sizes, classified as P16, P45, P63 and P100 (European Standard EN14961-1). The energy consumption and the price of wood chips usually increase with decreasing size. For the sake of simplicity and as a compromise between solid dynamic requirements and commercial availability, wood chips of 20mm nominal size were chosen. This size can be classified as the average size of the P45 class of the European Standard.

In order to evaluate the plant device sizing, the wood chips were further characterized by a particle density of 900 kg/m^3 and a bulk density of 400 kg/m^3.

The whole process is composed of five stages: air and biomass feeding, gasification, syngas clean-up and cooling, recycling, and electrical energy conversion as represented in figure 3.

Figure 3: Process block diagram

The biomass feeding system was assumed to be composed of an atmospheric hopper connected to a pressurized hopper, which fed a screw conveyor, through a rotary star valve. Using the model proposed by Dai and Grace 2008, the power consumption of the biomass feeding system was evaluated and it was so small as to be negligible.

The air for the gasification was taken from the environment and blown in the gasifying medium mixer using a proper blower.

The gasifier was designed as a square-section spouted bed with a pyramidal base. The main parameters of this device were calculated using the correlations listed in Appendix A and are summarized in table 3**Table 3.**

Table 3: Spouted bed gasifier parameters

The column side dimension, inlet diameter, base angle, base inlet side and cone height were designed according to correlations and best practice available in literature. The solid biomass residence time was estimated using the method proposed by Desappa et al. 2004 and the biomass content was consequently calculated. The inert (sand) mass fraction and content were fixed to a value which involves a sort of minimum for the spouting velocity. The annulus voidage was assumed equal to the loosely packing voidage, which was experimentally measured using few material sample (wood chips and sand mixtures). The static bed depth was calculated using solid mass content and its bulk density and the geometry of the spouted bed. The maximum spoutable height, the average spout diameter, the minimum spouting velocity and the stable spouting pressure drop were calculated using the correlations listed in Appendix A.

The syngas leaving the gasifier passes through the cyclone which produces a perfect ideal gas-solid separation by removing ash and carbon. The resulting syngas passes to the clean-up section, represented as a simple cooler with an outlet temperature of 130°C.

After that the syngas is cooled further and the condensable component can be removed in the syngas cooler-condenser. We chose 30°C as the outlet temperature of the syngas cooler-condenser as this value is easily reachable with either fresh water or with ambient-air cooling.

The recycling section was developed in order to reach stable spouting gas velocity in the spouted bed. Different configurations were tested in our simulations. A first configuration without recycles was tested and demonstrated the need for a supplementary gas source to be fed to the spouted bed for a stable spouting regime. Adding more air was found to oxidize the produced syngas too much

lowering its LHV. In a second configuration we tried to add low-pressure steam, but the heat cost for the steam production was too high for the plant power. A third configuration provided with flue-gas recirculation from the ICE was tested. Adding flue gases to the gasifier notably lowered the syngas LHV. This configuration could be exploited for a power generator that functions with a lean fuel, such as turbine gas. However, all of the tested configurations produced an outlet stream of syngas condensate. It was then proposed to recycle as much of the condensate as possible to reduce clean-up problems.

The plant configuration described in the block diagram of figure 3 was found to be the best of all the tested configurations for gasification in a spouted bed reactor for energy production. This configuration consists of syngas condensate recycling and hot syngas recycling. The condensate recycling was designed firstly to limit waste-water production that exceeded the battery limits. But complete condensate recycling is difficult to achieve, so the recycled condensate fraction is an important optimization parameter for the plant.

The hot syngas recycling was added to adjust the volumetric flow fed to the gasifier. So the mass flow of the syngas recycling was constrained by the volumetric flow feeding the spouted bed acting on the stream split fraction after the cyclone.

The condensate recycle and the syngas recycle contain combustible matter (methanol, phenol and naphthalene) that burns in the presence of hot air in the mixer before entering the spouted bed and in the inlet zone of the spout. So this recycling configuration should reduce the tar yield, but this desirable side effect could be confirmed only through a proper kinetic model of the gasifier.

The purified and cooled syngas coming from the syngas cooler-condenser is passed to the power section, where it is burnt in the ICE to produce heat and electricity.

5 Results

A first modelling and simulation step was performed in order to obtain a preliminary stream table and a screenshot of the unit operation conditions. Our preliminary results were used to design the apparatus. The main result of this sizing was the determination of the volumetric flow constraint needed for the spouted bed gasifier. A value of 120m^3/h was found to be conservative for a stable spouting regime.

Several important parameters can be simulated with the proposed model. The most important are the condensed recycle, and the air equivalent ratio, which directly influence the efficiency of the process, so they represent process optimization parameters. As mentioned before, the gasifier was modelled as an adiabatic reactor, but introducing the conservative gasification temperature of 930°C, ER and the condensate recycling were bound to that objective temperature.

Another parameter also influences the process behaviour: the quality of the feedstock. The dry biomass matter (organic matter and ash) composition is quite constant over a wide range of wood feedstocks, but the moisture can vary greatly. For this reason we studied the feedstock quality in terms of moisture content, varying this parameter from the ideal condition of 0%wt to the worst case of 35%wt moisture content in the biomass fed to the plant.

Many output variables can be monitored by the model, such as stream compositions and mass flows, pressures and temperatures, reaction conversions. For the scope of the process study, the focus was on the power and heat conversion. So the net power (electricity, cogeneration heat and total) yields referring to the biomass feed rate and biomass LHV were monitored together with the syngas quality in terms of syngas LHV.

Since the ER and condensate recycling are bound to the gasification temperature, it is possible to map a correspondence for the biomass moisture content as shown in figure 4. This map shows that for any given biomass moisture content, increasing the condensate recycling requires a greater amount of air to be able to reach the gasification temperature of 930°C. This trend has two limits. The first consists of a thermal limit: when a high proportion of the condensate is recycled it

becomes more difficult to reach the gasification temperature. The second consists of a mass balance limit: when too much condensate is recycled, the plant starts to accumulate a great amount of condensate until the steady state condition can not be longer found.

By increasing the biomass moisture content the exploitable region narrows in terms of condensate recycling. For the ideal 0%wt moisture content, it is possible to recycle all the condensate with a limited quantity of air, otherwise, for the worst-case 35%wt moisture content, only about 45% of the total condensate coming from the syngas cooler-condenser can be recycled, while burning out about half of the biomass feed (air ER = 50%).

Figure 4: Mapping of the recycled condensate fraction (recycled condensate over total condensate from the syngas cooler-condenser) and air ER for different biomass moisture fractions.

The production of the plant in terms of net electric yield was studied and figure 5 shows the plant performance variation against the air ER for various biomass moisture contents. Using the map in figure 4 the graph can be redrawn against the recycled condensate fraction. For the ideal 0% biomass moisture fraction a maximum net electrical yield of nearly 25% could be reached. Only for this ideal curve can a derivative sign change be noted at the ER value of 32%. The slight initial yield increment in this case is due to the favourable effect of water on the reforming reactions. After this maximum and for all other curves, increasing the air flow, or, similarly, increasing the condensate recycling, reduces the yield because of the higher combustion of the available LHV of the biomass. Moreover, increasing the biomass moisture content lowers the yield.

Figure 5: Net electrical energy yield vs. air ER for various biomass moisture fractions.

The heat cogeneration of the plant could be an interesting resource. As shown in figure 6, the cogeneration yield ranges are greater than corresponding electrical ones and it is possible to find a

maximum cogeneration yield for all biomass moisture fractions. The first yield increase is due to the increased raw syngas flowing through the clean-up section (the first cogeneration source). The succeeding yield decrease is due to the syngas LHV reduction and thus to the ICE total power reduction (the second cogeneration source). Air preheating seems to have little effect on the overall heat balance.

When the biomass moisture content is increased, the cogeneration yield decreases and the curves tend to flatten due to the heat required for vaporization.

Figure 6: Cogeneration yield vs. air ER for different biomass moisture fractions

The total yield of the plant can be obtained by summing the electrical and heat yields since both refer to the biomass feed energy content. To present the results from a different point of view, the total yield shown in figure 7 was traced against the recycled condensate fraction for different biomass moisture fractions. Increasing the biomass moisture fraction causes the total yield to decrease as considerable energy is consumed in the moisture vaporization.

For biomass moisture fractions ranging from 0%wt to 10%wt the total yield is low due to the cogeneration trend contribution. Above 10%wt biomass moisture content, the cogeneration yield trend flattens to produce the maximum in the total yield trend.

Figure 7: Total (heat and power) yield of the plant vs. the recycled condensate fraction for different biomass moisture fractions

6 Conclusions

The feasibility of a biomass gasification plant was studied using thermodynamic models, and considering the applicability of a spouted bed reactor as innovative technology. After a first process simulation, a preliminary estimation of the sizes of the plant devices was made, highlighting an important issue regarding the applicability of a spouted bed gasifier. While, on the one hand, the optimal thermodynamic conditions require a certain amount of air and/or steam, on the other hand, the spouting regime requires a constrained range of gas flows. This issue justifies the complex recycling system (syngas recycling and syngas condensate recycling) studied.

The introduction of the condensate recycling and the gasification temperature constraint of 930°C limited the plant parameters. Thus a plant functioning map was drawn for different biomass moisture fractions and considering the air ER and the recycled condensate fraction.

The plant power and heat yields were monitored to check the performance limits of our gasification plant configuration. An ideal value near to 25% of the net electrical efficiency was found to be reachable only for ideal dry biomasses. A wide range of values were found for the net electrical yield from the ideal maximum of 25% to a minimum of about 17% for the process conditions studied. The heat cogeneration yield was found to vary in the range 45-48% for all the process conditions studied.

Further investigations are needed for plant sizing and functioning in order to develop a complete economic feasibility study.

7 Acknowledgment

This work was carried out with the modelling support of Eng. Paolo Greppi (LIBPF, http://www.libpf.com) and the experience of Prof. Giorgio Rovero (DISMIC – Politecnico di Torino – Turin, Italy) in the field of spouted bed plant.

8 Notation

A	surface area (section area) $[m^2]$
C_D	drag coefficient
D_c	column diameter $[m]$
D_i	inlet diameter $[m]$
D_s	spout diameter $[m]$
d_p	particle diameter $[m]$
ER	Equivalent Ratio
F_D	particle drag force $F_D = C_D \frac{\pi}{8} \rho_g d_p^2 u_g^2$ [N]
$\mathbb{G}$	fluid mass flux in spouted bed referring to column diameter $\left[\frac{kg}{m^2 s}\right]$
g	gravitational constant = 9,8166 $\left[\frac{m}{s^2}\right]$
$\mathcal{H}_0$	static bed height in spouted bed $[m]$
$\mathcal{H}_a$	bed (annulus) height in spouted bed $[m]$
$\mathcal{H}_c$	cone height in spouted bed $[m]$
$\mathcal{H}_f$	height of fountain in spouted bed $[m]$
$\mathcal{H}_{fb}$	height of free board in spouted bed $[m]$
$\mathcal{H}_m$	maximum spoutable bed height $[m]$
$\mathcal{H}_{mf}$	minimum fluidization bed height $[m]$
HHV	Higher heating value
ICE	Internal Combustion Engine
LHV	Lower Heating Value
P	pressure $[Pa]$
p_j	partial pressure of i in gas phase $[Pa]$
ΔP_f	Fluidization gas pressure drop $[Pa]$
ΔP_{max}	Maximum bed pressure drop $[Pa]$
ΔP_s	Stable spouting pressure drop $[Pa]$
T	temperature $[K]$
U	Actual spouting velocity referring to column diameter [m/s]
U_t	Particle terminal settling velocity [m/s]
U_{mf}	Minimum fluidization velocity referring to column diameter [m/s]
U_{ms}	Minimum spouting velocity referring to column diameter [m/s]
U_i	gas velocity at the inlet of spouted beds [m/s]
$u_{sp,0,\mathcal{H}_a}$	particle velocity on the axis at the bed surface of spouted beds
V_{sp}	solid particle volume $[m^3]$

Greek letters

$\tan\gamma$	internal friction factor
ε	void fraction (gas phase fraction)
ε_{mf}	bed void fraction at minimum fluidization condition
ε_0	bed void fraction of static bed
ε_{ms}	bed void fraction at minimum spouting condition in spouted bed
$\varepsilon_{sp}\big\vert_{\mathcal{H}_a}$	spout voidage at the bed surface
η	yield - efficiency
Θ	particle sphericity coefficient
Θ	base diverging angle [°]
μ	gas viscosity [Pa·s]
ρ_{bp}	bulk density of solid particle $\left[\frac{kg}{m^3}\right]$
ρ_{sp}	solid particle density $\left[\frac{kg}{m^3}\right]$
ρ_g	gas phase density $\left[\frac{kg}{m^3}\right]$

Adimensional numbers

Re	Reynolds
Re_{mf}	Minimum fluidization Reynolds number $Re_{mf} = \frac{U_{mf} d_p \rho_g}{\mu}$
Re_t	Particle settling Reynolds number $Re_t = \frac{U_t d_p \rho_{sp}}{\mu}$
A_r	Archimedes $Ar = \frac{d_p^3 (\rho_{sp} - \rho_g) \rho_g g}{\mu^2}$

Appendix A

Table for conical-based spouted bed design

References

Aguado, R.; Olazar, M.; San Josè, M. J.; Aguirre, G. and Bilbao, J., 2000. Pyrolysis of Sawdust in a Conical Spouted Bed Reactor. Yields and Product Composition. Ind. Eng. Chem. Res. 39, 1925-1933.

Aguado, R.; Prieto, R.; José, M. J.; Alvarez, S.; Olazar, M. and Bilbao, J., 2005. Defluidization modelling of pyrolysis of plastics in a conical spouted bed reactor. Chemical Engineering and Processing: Process Intensification 44, 231 – 235.

Altzibar, H.; Lopez, G.; Alvarez, S.; San José, M.J.; Barona, A. and Olazar, M., 2005. A draft-tube conical spouted bed for drying fine particles. Drying Technology 26, 308 – 314.

Altzibar, H.; Lopez, G.; Aguado, R.; Alvarez, S.; San José, M.J. and Olazar, M., 2009. Hydrodynamics of conical spouted beds using different types of internal devices. Chemical Engineering and Technology 32, 463 – 469.

Amutio, M.; Lopez, G.; Artetxe, M.; Elordi, G.; Olazar, M. and Bilbao, J., 2012. Influence of temperature on biomass pyrolysis in a conical spouted bed reactor. Resources, Conservation and Recycling 59, 23 – 31.

Anabtawi, M., Z..A., N., Hilal, A., Al-Muftah, M., Khalaf, M., Leaper, C. and. Hastaoglu, M. A., 2005. A force balance model of a spouted bed for Darcy and non-Darcy flow in the annulus. Adv. Powder Technol. 6(1), 35-48.

Arabiourrutia, M.; Elordi, G.; Lopez, G.; Borsella, E.; Bilbao, J. and Olazar, M., 2012. Characterization of the waxes obtained by the pyrolysis of polyolefin plastics in a conical spouted bed reactor. Journal of Analytical and Applied Pyrolysis 94, 230 – 237.

Baratieri, M., Baggio, P., Fiori, L., and Grigiante, M., 2008. Biomass as an energy source: thermodynamic constraints on the performance of the conversion process. Bioresour. Technol. 99, 7063-7073.

Becker, H. A., 1961. An investigation of laws governing the spouting of coarse particles. Chem. Eng. Sci. 18, 245-262.

Bernocco, D., Greppi, P. and Arato, E., 2011. A novel approach to the biomass pyrolysis step and product lumping. Comput.-Aided Chem. Eng.. 29, 111-115.

Bi, H. T., 2004. A Discussion on Minimum Spout Velocity and Jet Penetration Length. Can. J. Chem. Eng. 82, 4-10.

Coltters, R. and Rivas, A.L., 2004. Minimum fluidation velocity correlations in particulate systems. Powder Technol. 147, 34-48.

Cui, H. and Grace, J. R., 2007. Fluidization of biomass particles: A review of experimental multiphase flow aspects. Chem. Eng. Sci. 62, 45-55.

Cui, H. and Grace, J. R., 2008. Spouting of biomass particles: a review. Bioresour. Technol. 99, 4008-4020.

Dai, J and Grace, J. R., 2008. A model for biomass screw feeding. Powder Technol. 186, 40-55.

Desappa, S., Paul, P. J., Mukunda, H., SRajan, N. K. S., Sridhar, G. and Sridhar, H. V., 2004. Biomass gasification technology - a route to meet energy needs. Curr. Sci. 87(7), 908-916.

Easterly, J. L. and Burnham, M., 1996. Overview of biomass and waste fuel resources for power production. Biomass and Bioenergy. 10(2-3), 79-92.

ECN, Energy r.C.o.t.N. 2010. Phyllis, database for biomass and waste. (http://www.ecn.nl/phyllis).

Epstein, N. and Grace, J. R., 2011. Spouted and spout-fluid beds. Cambridge: Cambridge University Press.

Ganser, G. H. 1993. A rational approach to drag prediction of spherical and nonspherical particles. Powder Technol. 77, 143-152.

Geldart, D. 1973. Type of fluidization. Powder Technol. 7, 285-292.

Goyal, H. B., Diptendu Seal, and Saxena, R. C., 2008. Bio-fuels from thermochemical conversion of renewable resources: A review. Renewable and Sustainable Energy. 12, 504-517.

Greppi, P., 2006. LIBPF: a library for process flowsheeting in C++. Proceeding of the International Mediterranean Modelling Multiconference. 435-440.

He, Y. L., Lim, C. J., and Grace, J. R., 1998. Hydrodynamics of Pressurized Spouted Bed. Can. J. Chem. Eng. 76, 695-702.

He, Y. L., Qin, S. Z., Lim, C. J. and Grace, J. R., 1994. Particle velocity profiles and solid flow patterns in spouted beds. Can. J. Chem. Eng. 72, 562-568.

Higman, C. and Burgt, van d.M., 2003. Gasification. 1st ed. Boston: Elsevier Gulf Professional Publishing.

IEA, Internationa E.A. 2011. Key World Energy Statistics. (www.iea.org).

Makibar, J., Fernandez-Akarregi, A.R., Alava, I., Cueva, F., Lopez, G. and Olazar, M., 2011. Investigations on heat transfer and hydrodynamics under pyrolysis conditions of a pilot-plant draft tube conical spouted bed reactor. Chem. Eng. Process. 50, 790-798.

Markowski, A. and Kaminski, W., 1983. Hydrodynamic characteristics of jet-spouted beds. Can. J. Chem. Eng. 61, 377–381.

Mathur, K. B. and Epstein, N., 1974. Spouted beds. 1st ed. New York: Academic Press inc.

Mathur, K. B. and Gishler, P. E., 1955. A technique for contacting gases with coarse solid particles. A.I.Ch.E. Journal. 1, 157-164.

Matsumura, Y. and Minowa, T., 2004. Fundamental design of a continuous biomass gasification process using a supercritical water fluidized bed. Int. J. Hydrogen Energy 29, 701–707.

Milne, T. A., Evans, R. J. and Abatzoglou, N., 1998. Biomass gasifier tars: their nature, formation and conversion. Golden: National Renewable Energy Laboratory.

Olazar, M.; Aguado, R.; Bilbao, J. and Barona, A., 2000. Pyrolysis of sawdust in a conical spouted-bed reactor with a HZSM-5 catalyst. AIChE Journal 46, 1025-1033.

Olazar, M., Lopez, G., Altzibar, H., Aguado, R. and Bilbao, J., 2009. Minimum Spouting Velocity Under Vacuum and High Temperature in Conical Spouted Beds. Can. J. Chem. Eng. 87, 541-546.

Olazar, M., San Jose, M. J., Izquierdo, M. A., Alvarez, S. and Bilbao, J., 2004. Fountain Geometry in Shallow Spouted Beds. Ind. Eng. Chem. Res. 43, 1163-1168.

Olazar, M., San Jose, M. J., LLamosas, R. and Bilbao, J., 1994. Hydrodynamics of sawdust and mixture of wood residues in conical spouted beds. Ind. Eng. Chem. Res. 33, 993-1000.

Prins, M. J. 2005. Thermodynamic analysis of biomass gasification and torrefaction, 1 ed. Eindhoven: Technische Universiteit Eindhoven.

Rasul, M. G., 2001. Spouted bed combustion of wood charcoal: performance comparison of three different designs. Fuel 80, 2189-2191.

Rovero, G. and Watkinson, A. P., 1990. A two-stage spouted bed process for autothermal pyrolysis or retorting. Fuel Process. Technol. 26 (3), 221-238.

Salam, P. A. and Bhattacharya, S. C., 2006 a. A comparative hydrodynamic study of two spouted bed reactor design. Chem. Eng. Sci. 61, 1946-1957.

Salam, P. A. and Bhattacharya, S. C., 2006 b. A comparative study of charcoal gasification in two types of spouted bed reactors. Energy. 31, 228-243.

San Jose, M. J., Olazar, M., Izquierdo, M. A., Alvarez, S. and Bilbao, J., 2001. Spout Geometry in Shallow Spouted Beds. Ind. Eng. Chem. Res. 40, 420-426.

San Josè, M. J., Olazar, M., Izquierdo, M. A., Alvarez, S. and Bilbao, J., 2004. Solid trajectories and cycle times in spouted beds. Ind. Eng. Chem. Res. 43, 3433-3438.

Sinnott, R. K., Coulson, J. M. and Richardson, J. F., 1999. Coulson and Richardson's Chemical Engineering: Chemical Engineering Design. 3rd ed. Oxford: Butterworth-Heinemann Ltd.

Souza-Santos, M. L., 2004. Solid fuels combustion and gasification. New York. Marcel Dekker, Inc.

Vassilev, S. V., Baxter, D., Andersen, L. K. and Vassileva, C. G., 2010. An overview of the chemical composition of biomass. Fuel. 89, 913-933.

Wu, S. M., Lim, C. J. and Epstein, N., 1987. Hydrodynamics of spouted beds at elevated temperatures. Chem. Eng. Commun. 62, 251-268.

Ye, B., Lim, C. J. and Grace, J. R., 1992. Hydrodynamics of Spouted and Spout-Fluidized Beds at High Temperature. Can. J. Chem. Eng. 70, 840-847.

Zahed, A. H. and Epstein, N., 1992. Batch and continuous spouted bed drying of cereal grains: the thermal equilibrium model. Can. J. Chem. Eng. 70, 945-953.

Figure 1: Spouted bed working scheme

Figure 2: Spouted bed geometry

Figure 3: Process block diagram

Figure 4: Mapping of the recycled condensate fraction (recycled condensate over total condensate from the syngas cooler-condenser) and air ER for different biomass moisture fractions.

Figure 5: Net electrical energy yield vs. air ER for various biomass moisture fractions.

Figure 6: Cogeneration yield vs. air ER for different biomass moisture fractions

Figure 7: Total (heat and power) yield of the plant vs. the recycled condensate fraction for different biomass moisture fractions

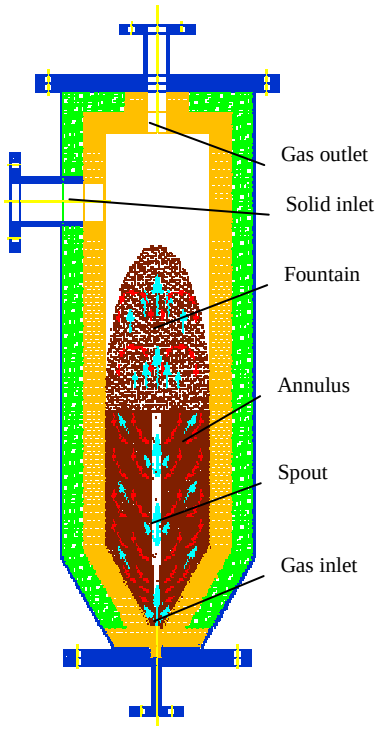

Figure 1: Spouted bed working scheme

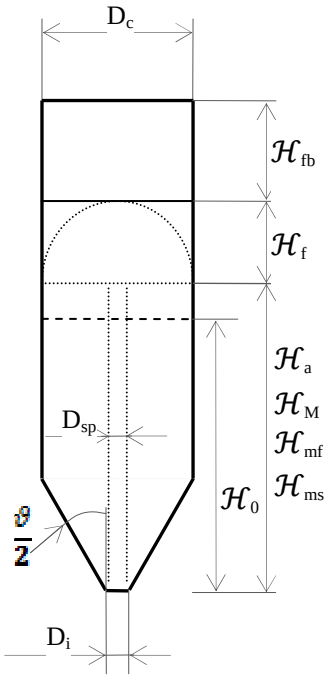

Figure 2: Spouted bed geometry

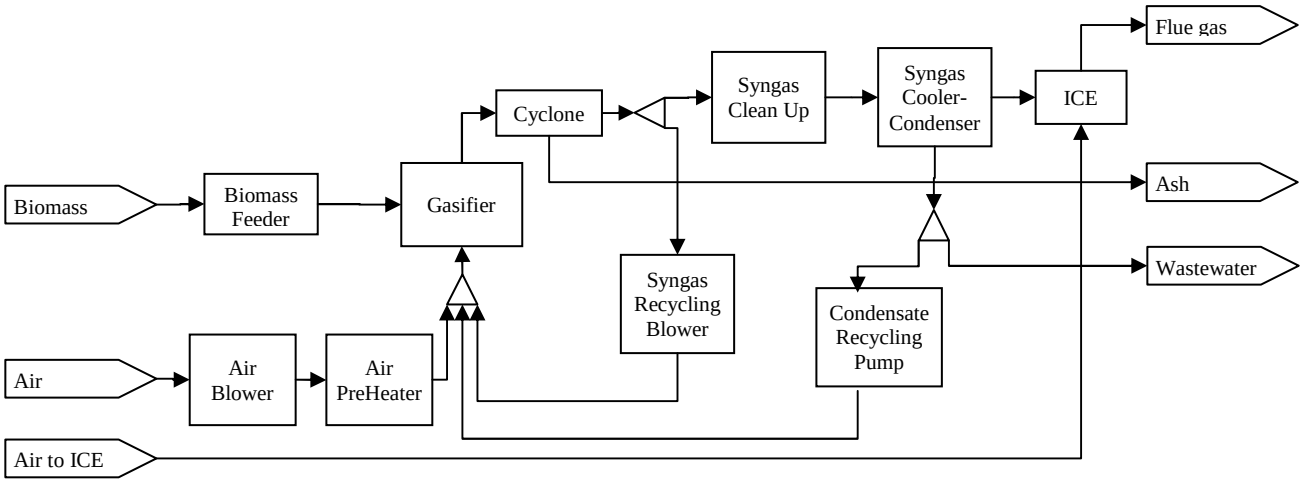

Figure 3: Process block diagram

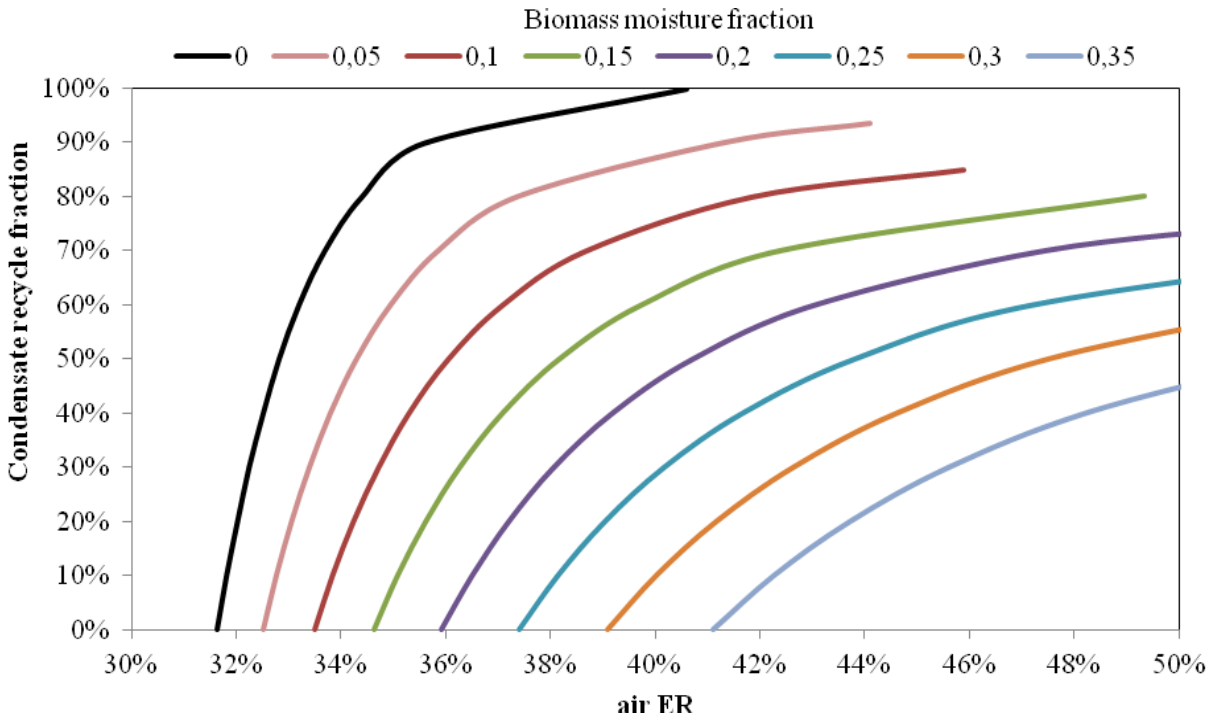

Figure 4: Mapping of the recycled condensate fraction (recycled condensate over total condensate from the syngas cooler-condenser) and air ER for different biomass moisture fractions.

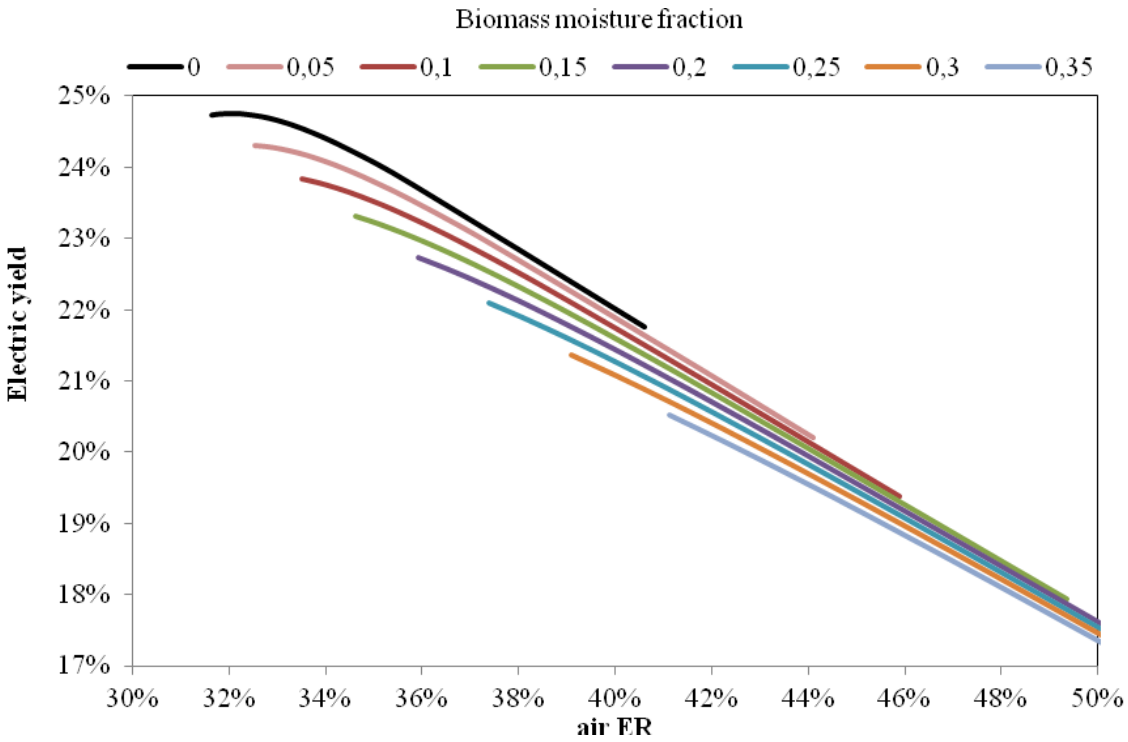

Figure 5: Net electrical energy yield vs. air ER for various biomass moisture fractions.

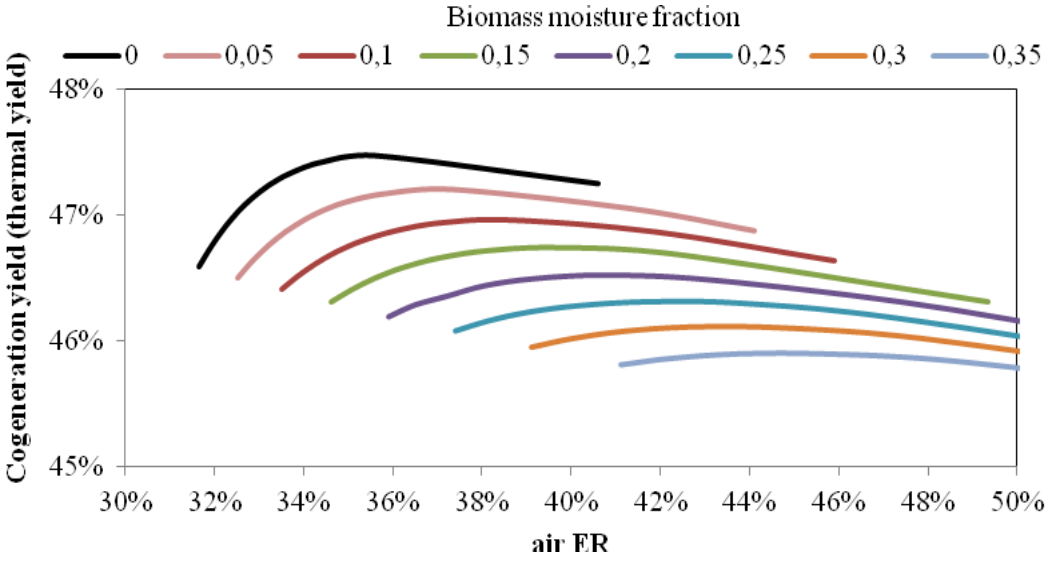

Figure 6: Cogeneration yield vs. air ER for different biomass moisture fractions

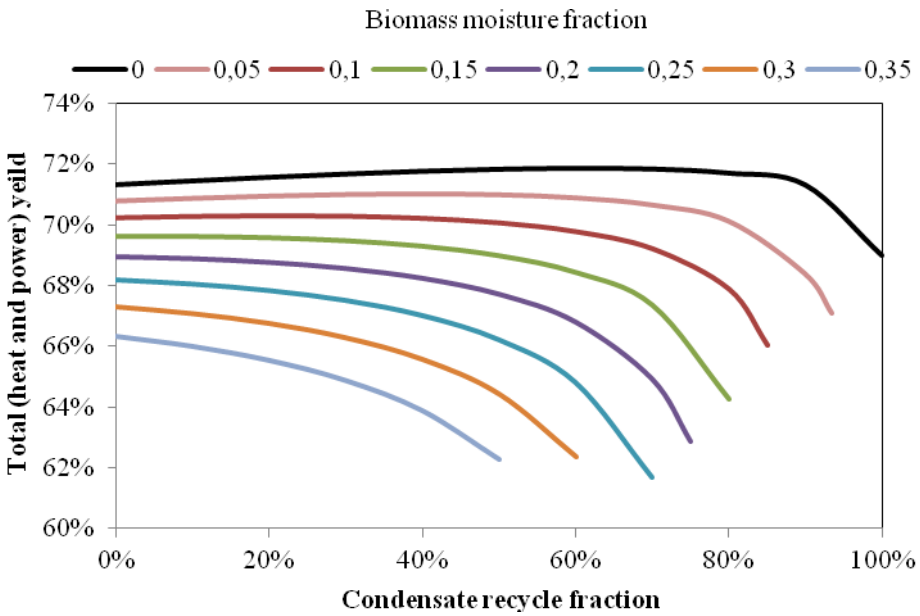

Figure 7: Total (heat and power) yield of the plant vs. the recycled condensate fraction for different biomass moisture fractions

Table 1: Chemical reactions considered

Table 2: Chemical characteristics of the biomasses (ECN 2010). HHV = higher heating value, LHV= lower heating value, M = moisture, VM = volatile matter, A = ash, FC = fixed carbon, ar = as received basis, dry = moisture-free basis, daf = dry and free ash.

Table 3: Spouted bed gasifier parameters

Appendix A: Table for conical-based spouted bed design

Table 1: Chemical reactions considered

Combustions		
	$CH_4 + 2O_2 \rightarrow CO_2 + 2H_2O$	(1)
	$H_2 + 0.5O_2 \rightarrow H_2O$	(2)
	$CO + 0.5O_2 \rightarrow CO_2$	(3)
	$C + O_2 \rightarrow CO_2$	(4)
	$NH_3 + 0.75O_2 \rightarrow 0.5N_2 + 1.5H_2O$	(5)
	$CH_3OH + 1.5O_2 \rightarrow CO_2 + 2H_2O$	(6)
	$C_2H_4 + 3O_2 \rightarrow 2CO_2 + 2H_2O$	(7)
	$C_6H_5OH + 7O_2 \rightarrow 6CO_2 + 3H_2O$	(8)
	$C_{10}H_8 + 12O_2 \rightarrow 10CO_2 + 4H_2O$	(9)
Equilibria		
	$CH_4 + H_2O \rightleftarrows CO + 3H_2$	(10)
	$0.5N_2 + 1.5H_2 \rightleftarrows NH_3$	(11)
	$CO_2 + H_2 \rightleftarrows CO + H_2O$	(12)
	$2CO \rightleftarrows CO_2 + C$	(13)
	$C + O_2 \rightleftarrows CO_2$	(14)
Reforming		
	$CH_3OH + H_2O \rightarrow CO_2 + 3H_2$	(15)
	$C_6H_5OH + 5H_2O \rightarrow 6CO + 8H_2$	(16)
	$C_{10}H_8 + 10H_2O \rightarrow 10CO + 14H_2$	(17)
	$C_2H_4 + 2H_2O \rightarrow 2CO + 4H_2$	(18)
Pyrolysis		
	$C_cH_hN_nO_o \rightarrow \upsilon_{H_2}H_2 + \upsilon_{O_2}O_2 + \upsilon_C C + \upsilon_{N_2}N_2 + \upsilon_{CO}CO + \upsilon_{CO_2}CO_2 + \upsilon_{H_2O}H_2O + \upsilon_{CH_4}CH_4 + \upsilon_{NH_3}NH_3 + \upsilon_{C_2H_4}C_2H_4 + \upsilon_{CH_3OH}CH_3OH + \upsilon_{C_6H_5OH}C_6H_5OH + \upsilon_{C_{10}H_8}C_{10}H_8$	(19)

Table 2: Chemical characteristics of the biomasses (ECN 2010).
HHV = higher heating value, LHV = lower heating value,
M = moisture, VM = volatile matter, A = ash, FC = fixed carbon,
ar = as received basis, dry = moisture-free basis, daf = dry and free ash.

Fuel	HHV [kJ/kg]			LHV [kJ/kg]			M [wt% ar]	Proximate composition [wt% dry]			Elemental composition [%wt daf]					
	Ar	dry	daf	ar	dry	daf		VM	A	FC	C	O	H	N	S	Cl
Oak wood, green whole tree chipped	11247	19392	19942	9126	17503	18000	42.0	80.5	2.8	16.7	50.4	39.7	8.9	0.50	0.50	-
Mixed hardwood chips	18690	19268	19448	17346	17958	18127	3.0	83.4	0.9	15.7	50.1	43.5	6.1	0.30	-	0.03
Sawdust wood	12630	19410	19618	10935	18115	18309	34.9	84.6	1.1	14.3	49.8	43.8	6.0	0.40	0.02	-
Park waste wood	18515	19520	20172	17211	18278	18888	5.2	77.6	3.2	19.2	51.2	42.5	5.9	0.26	0.05	0.06
Average	15271	19398	19795	13655	17964	18331	21.3	81.5	2.0	16.5	50.34	42.34	6.72	0.36	0.19	0.04

Table 3: Spouted bed gasifier parameters

Column side	0.266	m
Inlet diameter	0.030	m
Base angle	60	°
Base inlet side	0.040	m
Cone height	0.204	m
Biomass residence time	900	s
Biomass content	5.00	kg
Inert particle dimension	0.001	m
Inert mass fraction	0.75	
Inert content	15.00	kg
Annulus voidage	0.506	
Static bed depth	0.370	m
Maximum spoutable height	2.546	m
Average spout diameter	0.044	m
Minimum spouting velocity	0.464	m/s
Stable spouting pressure drop	3800	Pa

Appendix A

Conical-based spouted bed design

First Category: Dependence only from the properties of the gas and particles and process specification	Particle terminal settling velocity Ganser, (1993) correlation (Ganser 1993)	$C_D = \frac{24}{Re_t K_1}(1 + 0.112[Re_t K_1 K_2]^{0.657}) + \frac{0.4305 K_2}{1 + \frac{3305}{Re_t K_1 K_2}}$ $(Re_t K_1 K_2 < 10^5)$	$K_1 = \left(\frac{1}{3} + \frac{2}{3}\Theta^{-0.5}\right)^{-1}$ $K_2 = 10^{1.8148(-\log\Theta)^{0.5743}}$
	Biomass particle hold ups	Few minutes for little particle, such as sawdust. 15-20 minutes for bigger particle, such as wood chips The model proposed by Desappa et al.(Desappa et al. 2004) was used in the present work to estimate the residence time of wood chips	
	Minimum fluidization velocity Lippens and Mulder (1993) correlation (Coltters and Rivas 2004)	$\frac{Ar}{Re_{mf}} = f(\varepsilon_{mf}, \Theta) + g(\varepsilon_{mf}, \Theta) Re_{mf}$	$Re_{mf} = [C_1^2 + C_2 Ar]^{0.5} - C_1$ C1 = 27.2, C2 = 0.0408 recommended for high temperature conditions (Ye et al. 1992).
	Minimum fluidization velocity Wen and Yu correlation (Matsumura and Minowa 2004)	$Re_{mf} = [33.7^2 + 0.0408 Ar]^{0.5} - 33.7$	$U_{mf} = \frac{\mu Re_{mf}}{d_p \rho_g}$
Second Category: Dependence also from column geometry	Becker condition (Mathur and Epstein 1974)	$\left(\frac{D_i}{D_c}\right)_{min}$	0.35 for big particles, 0.1 for thin particles
	Spoutability, Chandnani and Epstein condition (Mathur and Epstein 1974)	$\frac{D_i}{d_p} < 25 \div 30$	Also valid for high temperature condition Wu et al. 1987.
	Stability, Littman condition (Mathur and Epstein 1974)	$\frac{D_c}{D_i} > 3 \div 12 \quad and \quad \mathcal{H}_a < \mathcal{H}_m$	
	Maximum spoutable bed height Malek and Lu equation (Mathur and Epstein 1974)	$\frac{\mathcal{H}_M}{D_c} = 0.105 \left(\frac{D_c}{d_p}\right)^{0.75} \left(\frac{D_c}{D_i}\right)^{0.4} \frac{\Theta^2}{\rho_{sp}^{1.2}}$ $(\rho_{sp}\ in\ [Mg])$	$\Theta = 0.205 \frac{A_p}{V_p^{2/3}}$ (shape factor) $D_c = 0.10 \div 0.23\ m \quad d_p = 0.8 \div 3.7 mm$
	Maximum spoutable bed height McNab and Bridgwater (1977) equation (Ye et al. 1992)	$\mathcal{H}_M = \frac{D_c^2}{d_p}\left(\frac{D_c}{D_i}\right)^{2/3} \frac{700}{Ar}[(1 + 35.9 \cdot 10^{-6} Ar)^{0.5} - 1]^2$	Suggested for high temperature conditions (Ye et al. 1992, Wu et al. 1987). It over predicts Hm at room condition. The over prediction reduces increasing temperature. At ~800 °C, the over prediction is ~30%.
	Static bed height	Height deriving from solid residence time, solid bulk density in static condition and column geometry	
	Average spout diameter Bridgwater and Mathur (1972) equation (Mathur and Epstein 1974)	$D_s = \frac{0.384\, \mathbb{G}^{0.50}\, D_c^{0.75}}{\rho_{bp}^{0.25}}$	
	Average spout diameter Wu et al (1987) equation (Mathur and Epstein 1974)	$D_s = \frac{5.61\, \mathbb{G}^{0.433}\, D_c^{0.583} \mu^{0.133}}{(\rho_{bp} \rho_g g)^{0.283}}$	Suggested for high temperature conditions (Wu et al. 1987). It under exstimates Ds of ~30% (Ye et al. 1992)
Third Category: Dependence also from bed depth	Minimum spouting velocity Mathur and Gishler (1955) equation (Mathur and Gishler 1955)	$U_{ms} = (2g\mathcal{H}_0)^{0.5} \left(\frac{d_p}{D_c}\right) \left(\frac{D_i}{D_c}\right)^{0.33} \left(\frac{\rho_{sp} - \rho_g}{\rho_g}\right)^{0.5}$	$D_c = 0.14 \div 1.1\ m \quad \vartheta = 60° \quad \frac{H_0}{D_c} = 1.0 \quad \frac{D_i}{D_c} = 1/6$ $d_p = 2.5 \div 3.5 mm \quad T = 30°C$
	Minimum spouting velocity Wu et al (1987) equation (Wu et al. 1987)	$U_{ms} = 10.6(2g\mathcal{H}_0)^{0.5} \left(\frac{d_p}{D_c}\right)^{1.05} \left(\frac{D_i}{D_c}\right)^{0.266} \left(\frac{\mathcal{H}_0}{D_c}\right)^{-0.095} \left(\frac{\rho_{sp} - \rho_g}{\rho_g}\right)^{0.256}$	Suggested for high temperature conditions. It usually under predicts Ums by ~10% (Ye et al. 1992, Wu et al. 1987)
	Fountain height Grace and Mathur (1978) theorical model (He et al. 1994)	$\mathcal{H}_f = \left(\varepsilon_{sp}\big\vert_{\mathcal{H}_a}\right)^{1.46} \frac{\left(u_{sp,0,\mathcal{H}_a}\right)^2}{2g} \frac{\rho_{sp}}{\rho_{sp} - \rho_g}$	
	Fountain height Day theorical model (Olazar et al. 2004)	$\frac{\mathcal{H}_f}{D_i} = 46.4 \left(\frac{U}{U_{ms}} - 1\right)^{0.865} \left(\frac{\mathcal{H}_a}{\mathcal{H}_M}\right)^{-0.379} \left(\frac{\rho_g}{\rho_{sp} - \rho_g} \frac{U_{mf} U_{pt}}{g D_i}\right)^{2.13} \left(\frac{\rho_{sp} - \rho_g}{\rho_g}\right)^{-0.892} \left(\frac{d_p}{D_i}\right)^{-3.49} \left(\frac{D_i}{D_c}\right)^{-2.75}$	
	Maximum bed pressure drop Manurung, (1964) equation (Mathur and Epstein 1974)	$-\frac{\Delta P_{max}}{g \rho_b \mathcal{H}_a} = \left[\frac{6.8}{\tan\gamma} + 0.80\right] - 34.4 \frac{d_p}{\mathcal{H}_a}$	
	Stable bed pressure drop Manurung, (1964) equation (Mathur and Epstein 1974)	$-\Delta P_s = \frac{g \rho_{bp} \mathcal{H}_0}{1 + \frac{0.81(\tan\gamma)^{1.5}}{\psi^2}\left(\frac{D_c d_p}{D_i}\right)^{0.78}\left(\frac{D_c}{\mathcal{H}_0}\right)}$	$\psi = \frac{d_p}{d(same\ vol.\ spherical\ particle)}$ Suggested also for high temperature conditions (Wu et al. 1987)